



Surface Science Letters

Correlating STM contrast and atomic-scale structure by chemical modification: Vacancy dislocation loops on FeO/Pt(1 1 1)

L.R. Merte^a, J. Knudsen^a, L.C. Grabow^b, R.T. Vang^a, E. Lægsgaard^a, M. Mavrikakis^b, F. Besenbacher^{a,*}^a Interdisciplinary Nanoscience Center (iNANO), Department of Physics and Astronomy, University of Aarhus, Ny Munkegade Building 520, DK-8000 Aarhus C, Denmark^b Department of Chemical and Biological Engineering, University of Wisconsin-Madison, Madison, Wisconsin 53706, USA

ARTICLE INFO

Article history:

Received 31 October 2008

Accepted 5 November 2008

Available online 28 November 2008

Keywords:

Scanning tunneling microscopy

Surface electronic phenomena

Reduction

Iron

Oxides

Thin film structure

Moiré superstructure

ABSTRACT

By chemically modifying the FeO(111) thin film on Pt(111), we show that it is possible to unambiguously correlate its STM morphology with its underlying structure without recourse to STM simulations. Partial reduction of the oxide surface leads to the formation of triangularly-shaped oxygen vacancy dislocation loops at specific sites in the moiré structure of the film. Their presence allows unambiguous identification of the high-symmetry domains of the moiré structure, whose differing chemical properties govern the templating effect on adsorbed metal atoms, clusters and molecules.

© 2008 Elsevier B.V. All rights reserved.

Epitaxial thin films with nanometer-scale structural dimensions have received significant attention in recent years due to their application as templates for the bottom-up assembly of regular arrays of nanostructures [1–3]. In the case of metal growth, preferential adsorption sites arranged periodically on the surface act as nucleation centers, allowing periodic arrays of monodisperse clusters to be grown simply by deposition of the component material under appropriate conditions.

Oxide thin films exhibiting moiré-type coincidence structures represent an important general class of materials for this application (see Ref. [4] and references therein). Since the symmetry and periodicity of these nanostructures are determined by the respective symmetries and lattice parameters of the oxide film and the substrate, different metal/metal oxide combinations, which potentially allow tunability of the geometric and adsorption properties, can be chosen.

Understanding the templating effects of these films is difficult, however. The variation in adsorption strength across the moiré superstructure is caused by subtle differences in the local atomic-scale structure of the metal/metal oxide interface and is therefore impossible to predict simply upon inspection, especially if no precise structural model is available. Experimental determination of the preferred adsorption sites using scanning probe microscopy is also in principle very challenging, as the apparent heights

observed in, for example, STM constant current topographs reflect a rather complicated convolution of the geometrical and electronic effects and thus cannot be correlated with the local structure of the film in a straightforward manner. In the past, the moiré-structured FeO(111) thin film on Pt(111) has been extensively characterized and its usefulness as a template for growth of metal particles [4,5] and molecules [6] has been demonstrated. So far the correlation between recorded STM topographs and the detailed local structure of this oxide film has been based on theoretically simulated STM topographs and work function measurements [7–9].

Chemical modification has proven to be a useful method for the interpretation of STM contrast. For example, differences in binding affinity of adsorbates for different elements have been used to distinguish chemical species on oxide [10] and bimetallic [11] surfaces. Reduction by CO has also been used to determine the number of Ag atoms incorporated in the p(4 × 4)-O structure on Ag(111) [12]. Here, we apply chemical modification in a novel way, and show that the atomic-scale structure of the thin FeO(111) film, including its local registry with the substrate, can be correlated unambiguously with experimentally recorded STM images independent of the tip state, which we find to have a strong impact on measured constant current STM topographs. By mildly reducing the film with atomic hydrogen, we produce oxygen vacancy dislocation loops whose size, orientation and location on the surface are found to be directly related to the moiré structure of FeO(111) and which therefore act as guideposts in STM images of the film. The importance of this approach is highlighted by the

* Corresponding author. Tel.: +45 8942 3604/3711; fax: +45 8612 0740.
E-mail address: fbe@inano.dk (F. Besenbacher).

disagreement between our findings and previous theoretical predictions. We find that FCC domains, and not the HCP domains, exhibit the highest local work function, implying that these are the preferred adsorption sites for Au atoms and MgPc molecules [5,6,8,13].

Measurements were made using a home-built Aarhus STM [14], with a mechanically cut Pt/Ir tip, mounted in an ultra-high vacuum chamber (base pressure: $\sim 1 \times 10^{-10}$ mbar). High-bias measurements were made at ~ 150 K, all others at room temperature. The Pt(111) surface was cleaned by cycles of Ar^+ bombardment and annealing at 1000 K. The FeO film was prepared by stepwise deposition and oxidation (1.3×10^{-6} mbar O_2 , 870 K, 2 min) of sub-monolayer quantities of Fe until a closed monolayer was formed. The film was found by STM to be well-ordered with few defects. Reduction of the film was accomplished by exposure to atomic hydrogen at room temperature using a commercial source (Oxford Applied Research TC-50). The background H_2 pressure during exposure was 2.7×10^{-8} mbar. Subsequent to STM measurements, the orientation of the Pt single-crystal as mounted in the sample holder was determined by Laue diffraction.

Spin polarized density functional theory calculations using the DFT + U approach by Dudarev [15] with $U = 4$ eV and $J = 1$ eV [8] on the FeO(111)/Pt(111) system were performed using the VASP total energy code [16,17]. Similar to a previous study on this system, we used the projector augmented wave (PAW) method with a kinetic energy cutoff of 400 eV combined with the PW91 exchange-correlation functional [18] and chose anti-ferromagnetic initial guesses for the magnetic moment of Fe atoms [8]. Commensurate 2×2 unit cells with the FeO film supported on 5 layers of Pt were employed to estimate the stabilities of the three high-symmetry domains (Top, HCP, FCC). We used both the theoretical lattice constant for Pt of 3.99 Å (Fe-Fe spacing = 2.82 Å) and an expanded Pt lattice, giving the experimentally determined value of the Fe-Fe distance of 3.09 Å, and relaxed the FeO film and the top two layers of Pt only in the z direction. The Brillouin zone was sampled using a $6 \times 6 \times 1$ Monkhorst-Pack k -point mesh.

The basic structure of the 1 ML FeO(111)/Pt(111) film, determined through STM, LEED and X-ray photoelectron diffraction studies [19–21], is shown in Fig. 1. The iron lattice has an average spacing of 3.1 Å (about 11% larger than the Pt–Pt spacing) and is slightly rotated relative to the substrate, giving rise to a $\sim 25^\circ$ moiré superstructure.¹ The surface is oxygen-terminated, and the placement of the O layer follows the fcc stacking sequence of the substrate so that a single orientation is preferred, with oxygen occupying only one of the two hollow sites of the Fe lattice in all domains.

As will be described in more detail in a future publication [22], exposure of the FeO film to atomic hydrogen at room temperature leads initially to the formation of surface hydroxyls (see also Ref. [23]), which can be imaged with STM and appear most often as bright protrusions. The concentration of these hydroxyls increases with exposure time until a threshold of $\sim 12\%$ ML, at which point reduction of the oxide film begins, evidenced by the formation of triangular features in STM images. Well-ordered triangles are also found to form upon heating the hydroxylated surface (also below the threshold coverage) briefly to 500 K, causing surface hydrogen to desorb as H_2 and H_2O [23].

The triangular features formed upon heating the hydroxylated surface are found in two types, distinguished by their size and location relative to the moiré structure (see Fig. 2a). All triangles of one

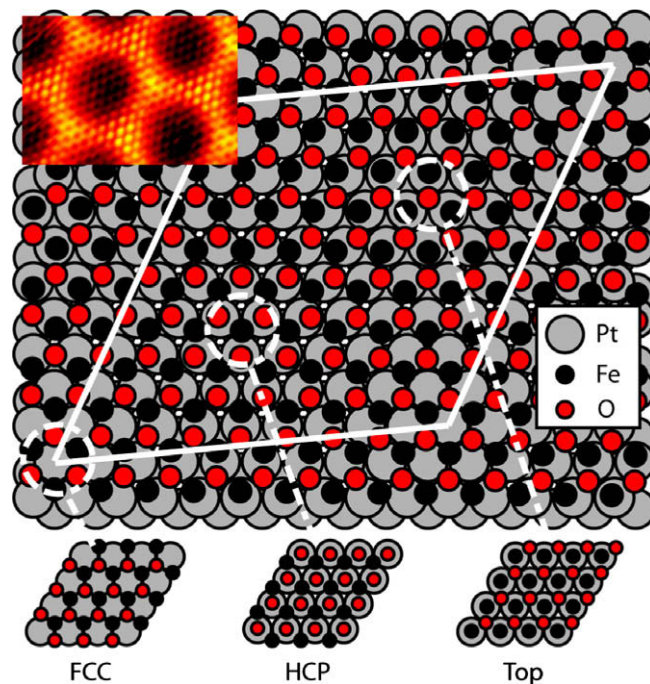


Fig. 1. Ball model of the structure of the film, showing the three high-symmetry domains found within the moiré cell. The approximate $\sqrt{91} \times \sqrt{91} 5.2^\circ$ unit cell is drawn. Inset: STM image of the film ($60 \times 40 \text{ \AA}^2$, 0.87 nA, 4 mV).

type are centered at a particular domain in the moiré structure and all are oriented in the same direction. In the following, we describe the structure of these triangles, which explains their orientation, followed by their location with respect to the moiré film.

Fig. 2b and c show STM images of two similar triangles obtained in different tip-dependent imaging modes. In both cases, atomic features are resolved, and registry analysis indicates that different chemical species are imaged. In Fig. 2b, the protrusions within the triangle are in registry with respect to the surrounding film and the atoms at the triangle edges appear to be missing. In Fig. 2c, on the other hand, we see that the protrusions within the triangle are out of registry with the surrounding film, suggesting the formation of a vacancy dislocation loop. It is apparent that, in the formation of the triangular features, one of the two types of atoms (Fe or O) shifts its position, while the other remains in place. We determine that the oxygen atoms are those that are shifted by imaging the surface after exposure to hydrogen but before heating, so that hydroxyl groups, which serve as labels for the O atoms, remain on the surface, as shown in Fig. 2d. Hydroxyl groups within the triangular domains are found to be shifted out of registry with those outside the triangles, just as the protrusions are in Fig. 2c.

A schematic model for the triangular features, implied by these STM measurements, is shown in Fig. 2e. In this case, which corresponds directly to the triangles shown in Fig. 2b,c, removal of 7 O atoms enables a group of 21 remaining O atoms to move to adjacent hollow sites in the Fe lattice. Note that the absence of protrusions along the triangle edges in Fig. 2b does not necessarily imply that Fe atoms have been removed, but is more likely an electronic effect caused by the change in coordination environment of these atoms. Migration of Fe into the Pt substrate appears highly unlikely, as the triangular features, though more well-ordered after brief annealing at 500 K, are formed at room temperature, where mixing between Pt and Fe is slow [24]. Huang and Ranke also observed no detectable loss of Fe from the surface following extensive reduction by atomic hydrogen [23]. We propose that the lateral positions of the Fe atoms at the triangle edges are unchanged (and hence become two-fold coordinated) following the

¹ Slightly different structures of the first FeO layer are formed for films with thicknesses below and above 1 ML, respectively. For thicknesses close to 1 ML, we observe some variability in the moiré parameters, with the unit cell dimensions varying between 24–26 Å, and rotation angles between 0° and 6° . Neither these variations, nor distortions of the film in the vicinity of steps and defects, are found to affect any of the trends we have observed.

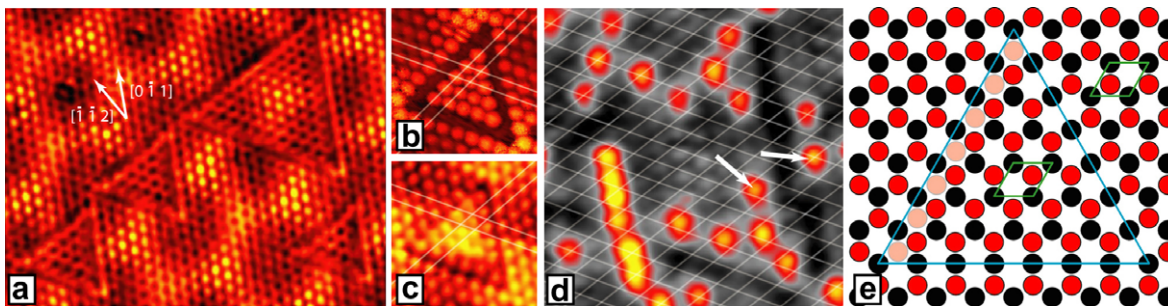


Fig. 2. (a) STM image ($92 \times 72 \text{ \AA}^2$, 2.5 nA, 10 mV) of the partially-reduced film, showing three small triangles and one large triangle. (b) Iron-mode STM image ($30 \times 30 \text{ \AA}^2$, 1.04 nA, 19.5 mV) showing one of the smaller triangular features. (c) Oxygen-mode STM image ($30 \times 30 \text{ \AA}^2$, 0.52 nA, 6.4 mV) showing one of the smaller triangular features. (d) STM image ($40 \times 40 \text{ \AA}^2$, 0.59 nA, 43.6 mV) of the FeO film after exposure to atomic hydrogen prior to heating, showing OH groups inside and outside a triangle. A high-contrast color scale is used to highlight the positions of the OH groups. The grid is based on the positions of OH groups found outside any triangles. Note the registry shift of the OH groups within the triangle. (e) Ball model corresponding to the triangles shown in (b) and (c). Pale red atoms show schematically the 7 oxygen atoms that have been removed.

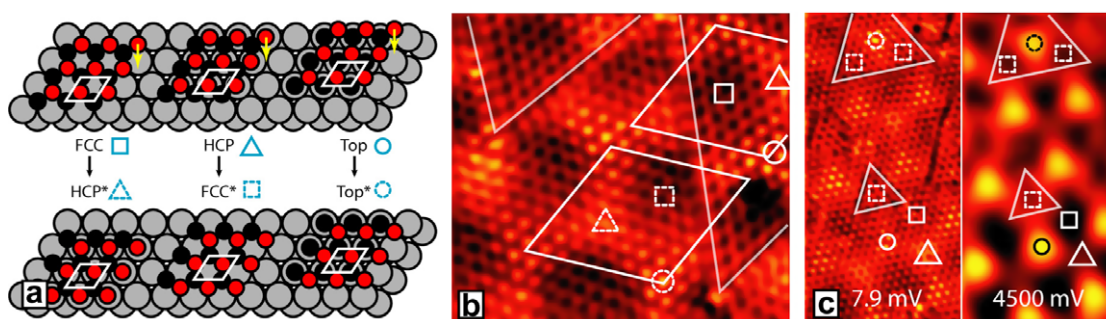


Fig. 3. (a) Schematic illustration of the effect of shifting the oxygen lattice at each of the high-symmetry domains of the moiré structure. (b) STM image ($55 \times 50 \text{ \AA}^2$, 1.08 nA, 8.2 mV) of a domain boundary separating two regions of opposite orientation. (c) STM images ($60 \times 120 \text{ \AA}^2$, 1.22 nA) of the same region of the surface taken at low (7.9 mV) and high (4500 mV) bias, respectively. Top and Top* domains are imaged brightest while FCC and FCC* domains are darkest in the high-bias image. Different symbols indicate the locations of different types of domains, as defined in (a), and are chosen to match those used in Refs. [7,8].

shift of the O atoms, as any shift in the edge Fe positions would be expected to have a detectable influence on the positions and appearance in STM of neighboring Fe and O atoms. Such a shift would further be expected to be energetically less favorable, as this would require an increase in Fe–O bond lengths and a decrease in Fe–Fe spacings, both of which are maintained in the present model.

To determine the locations of the triangles relative to the moiré structure, we examine the change in STM morphology accompanying the shift of the oxygen lattice. As shown in Fig. 3a, moving the oxygen atoms from one hollow site in the Fe lattice to the other changes the stacking sequence of the film's atomic layers, effectively inverting the orientation of the FeO film. The result is that an FCC domain is converted to an HCP-like domain (denoted HCP*) and an HCP domain to an FCC-like domain (FCC*). The Top domain is unchanged (Top*), as the oxygen atoms are shifted from one Pt hollow site to the other. If the effect of the atoms in the second Pt layer and below is assumed to be negligible, FCC domains and HCP domains should appear in STM images to have swapped, while Top domains should be unchanged in appearance.

Fig. 3b shows the contrast reversal across the boundary of an uncommonly large domain of inverted orientation. It can be seen that the appearance of one type of domain, showing the brightest, most well-defined protrusions, is retained across the boundary, and is thus assigned Top/Top*. The other two domains, imaged with lowest and intermediate apparent heights, respectively, have been reversed, consistent with the expected FCC \rightarrow HCP* and HCP \rightarrow FCC* shifts. This behavior is also observed in high bias (4500 mV) images where contrast is determined by variation in the local work function of the surface (Fig. 3c) and where the effect of deeper Pt layers is expected to be small. The Top domains are imaged bright-

est at high bias, in agreement with previous predictions [7,8], and do not change upon inversion. They are found always at the center of large triangles and along the edges of the smaller ones, so that the smaller triangles must, in light of the film's orientation (indicated by the orientation of the triangles), be centered at HCP domains.

This assignment, together with the fixed orientation of the triangles with respect to that of the film, enables us to locate the FCC, HCP and Top domains of the moiré structure in any imaging mode where the misfit dislocations can be resolved. One observation, based on this new result, is that the local work function of the surface is highest (imaged with the lowest apparent height at high bias) at FCC domains, in disagreement with expectations from a simple hard-sphere model and with computations based on larger, and apparently more realistic, non-pseudomorphic models [7,8]. This implies that the preferred adsorption sites for Au atoms and MgPc molecules are not HCP domains, as has previously been reported [5,6,13], but FCC domains.

The driving force for the formation of these triangular features, as well as their observed sizes, can be easily understood if one considers the relative stability of the FeO film in the different domains of the moiré structure. Our DFT calculations in a 2×2 unit cell, using both the normal and expanded lattice constants, indicate that its stability increases in the order Top \approx Top* < HCP \approx HCP* < FCC \approx FCC*, with the FCC-type domains being most stable.²

² Calculated energies, in eV per FeO unit, of the different domains relative to the FCC domain: (Fe–Fe 3.09 Å) FCC 0, FCC* –0.015, HCP 0.170, HCP* 0.200, Top 0.219, Top* 0.212. (Fe–Fe 2.82 Å) FCC 0, FCC* 0.032, HCP 0.133, HCP* 0.127, Top 0.377, Top* 0.375.

Partial reduction of the surface thus allows oxygen atoms, at the center of small triangles and the corners of large triangles, to shift from less favorable sites above Pt atoms to more favorable hollow sites, converting HCP domains to FCC domains and yielding an energy gain on the order of 0.1–0.2 eV per FeO unit.

Similar trends in structural stability are to be expected for all moiré-structured oxide films, suggesting that our method may find application beyond the FeO(111)/Pt(111) system. Indeed, we observe similar dislocations upon reduction of FeO films grown on Pd(111) and Au(111). In addition to their use as nanotemplates for the bottom-up assembly of regular arrays of nanostructures, these oxide films may serve as useful models for low-temperature oxidation catalysts, as noble metals in close contact with iron oxides have been shown to have high activities [25–27]. In such noble metal/reducible oxide catalysts, the oxide is believed to play a direct role in the catalytic mechanism. A promising approach to the study of these types of catalysts is the use of thin oxide films and nanostructures grown on flat metal substrates as model systems [28,29]. One of the main advantages of this method is that it simplifies atomic-scale imaging and allows detailed characterization of the metal/metal oxide interface and its physical and chemical properties. Application of FeO films as model catalysts will require accurate interpretation of STM images, the basis for which is provided by our work.

In conclusion, we have presented a new approach by which the STM images and their relation to the atomic-scale structure of an FeO thin film can be interpreted unambiguously. Our results deviate from recent theoretical studies, highlighting the delicate nature of the properties of the FeO film and emphasizing the need for experimental corroboration of theoretical results. The novel approach presented here should be generally applicable for the determination of the atomic-scale structure of many other thin epitaxial oxide films.

Acknowledgement

Work at UW was supported by DOE-BES, Chemical Sciences Division. Supercomputing time was utilized at NERSC, PNNL, and ORNL.

References

- [1] H. Brune, M. Giovannini, K. Bromann, K. Kern, *Nature* 394 (6692) (1998) 451–453.
- [2] M. Corso, W. Auwärter, M. Muntwiler, A. Tamai, T. Greber, J. Osterwalder, *Science* 303 (5655) (2004) 217–220.
- [3] S. Degen, C. Becker, K. Wandelt, *Faraday Discuss.* 125 (2004) 343–356.
- [4] N. Berdunov, G. Mariotto, K. Balakrishnan, S. Murphy, I.V. Shvets, *Surf. Sci.* 600 (21) (2006) L287–L290.
- [5] N. Nilius, E.D.L. Rienks, H.P. Rust, H.J. Freund, *Phys. Rev. Lett.* 95 (2005) 066101.
- [6] X. Lin, N. Nilius, *J. Phys. Chem. C* 112 (39) (2008) 15325–15328.
- [7] E.D.L. Rienks, N. Nilius, H.P. Rust, H.J. Freund, *Phys. Rev. B* 71 (24) (2005) 241404(R).
- [8] L. Giordano, G. Pacchioni, J. Goniakowski, N. Nilius, E.D.L. Rienks, H.J. Freund, *Phys. Rev. B* 76 (7) (2007) 075416.
- [9] H.C. Galloway, P. Sautet, M. Salmeron, *Phys. Rev. B* 54 (16) (1996) R11145–R11148.
- [10] H. Onishi, Y. Iwasawa, *Chem. Phys. Lett.* 226 (1–2) (1994) 111–114.
- [11] J. de La Figuera, J.E. Prieto, G. Kostka, S. Müller, C. Ocal, R. Miranda, K. Heinz, *Surf. Sci.* 349 (1) (1996) L139–L145.
- [12] M. Schmid, A. Reicho, A. Stierle, I. Costina, J. Klikovits, P. Kostelnik, O. Dubay, G. Kresse, J. Gustafson, E. Lundgren, J.N. Andersen, H. Dosch, P. Varga, *Phys. Rev. Lett.* 96 (2006) 146102.
- [13] L. Giordano, G. Pacchioni, J. Goniakowski, N. Nilius, E.D.L. Rienks, H.J. Freund, *Phys. Rev. Lett.* 101 (2008) 026102.
- [14] E. Laegsgaard, F. Besenbacher, K. Mortensen, I. Stensgaard, *J. Microsc.-Oxford* 152 (1988) 663–669.
- [15] S.L. Dudarev, G.A. Botton, S.Y. Savrasov, C.J. Humphreys, A.P. Sutton, *Phys. Rev. B* 57 (3) (1998) 1505–1509.
- [16] G. Kresse, J. Hafner, *Phys. Rev. B* 47 (1) (1993) 558(R)–561(R).
- [17] G. Kresse, J. Furthmüller, *Phys. Rev. B* 54 (16) (1996) 11169–11186.
- [18] J.P. Perdew, J.A. Chevary, S.H. Vosko, K.A. Jackson, M.R. Pederson, D.J. Singh, C. Fiolhais, *Phys. Rev. B* 46 (11) (1992) 6671–6687.
- [19] H.C. Galloway, J.J. Benitez, M. Salmeron, *Surf. Sci.* 298 (1) (1993) 127–133.
- [20] Y.J. Kim, C. Westphal, R.X. Ynzunza, H.C. Galloway, M. Salmeron, M.A. VanHove, C.S. Fadley, *Phys. Rev. B* 55 (20) (1997) R13448–R13451.
- [21] M. Ritter, W. Ranke, W. Weiss, *Phys. Rev. B* 57 (12) (1998) 7240–7251.
- [22] L.R. Merte, J. Knudsen, L.C. Grabow, R.T. Vang, E. Laegsgaard, M. Mavrikakis, F. Besenbacher, (in preparation).
- [23] W.X. Huang, W. Ranke, *Surf. Sci.* 600 (4) (2006) 793–802.
- [24] D.I. Jerdev, B.E. Koel, *Surf. Sci.* 513 (1) (2002) L391–L396.
- [25] M. Haruta, T. Kobayashi, H. Sano, N. Yamada, *Chem. Lett.* 16 (2) (1987) 405–408.
- [26] A.V. Kalinkin, V.I. Savchenko, A.V. Pashin, *Catal. Lett.* 59 (2–4) (1999) 115–119.
- [27] X.S. Liu, O. Korotkikh, R. Farrauto, *Appl. Catal. A* 226 (1–2) (2002) 293–303.
- [28] J.A. Rodriguez, S. Ma, P. Liu, J. Hrbek, J. Evans, M. Perez, *Science* 318 (5857) (2007) 1757–1760.
- [29] J. Schoiswohl, M. Sock, Q. Chen, G. Thornton, G. Kresse, M.G. Ramsey, S. Surnev, F.P. Netzer, *Top. Catal.* 46 (1–2) (2007) 137–149.